Multiscale finite element analysis of a porous heat exchanger

Roni Koitermaa

December 18, 2020

Abstract

A cylindrical heat exchanger with a porous medium is modelled numerically at different scales. Heat and fluid flow for the whole heat exchanger is modelled using values for porosity, permeability and thermal conductivity, which are determined at the microscale by simulating a unit cell of the porous material. An optimal microstructure for high heat transfer and low pressure drop is determined. This was found to consist of particles with their longest axis in the direction of heat flow and their shortest axis normal to the fluid flow.

1 Introduction

Numerical modelling can be used to determine the physical properties of materials at a wide range of scales. This can be useful in understanding how microscale properties influence the material at a larger scale. In this work this is applied to a heat exchanger that uses a porous medium to transfer heat between fluids. Properties of the porous medium can be determined from the microscale structure by simulating fluid flow and heating processes.

2 Macroscale reference solution with no porous medium

The heat exchanger was constructed in COMSOL as a 2D axisymmetric model. The hot and cold air channels are concentric cylinders with a total length of 50 cm and radii $r_{\text{hot}} = 2$ cm, $r_{\text{cold}} = 3$ cm and $R_{\text{cold}} = 4$ cm. In the middle of the heat exchanger the cold and hot channels are connected by solid aluminium.

The simulation of the heat exchanger requires simulation of both fluid motion and heat. Heat simulation is performed using the *Heat Transfer in Porous Media* module, but with no porous medium. Thermal insulation is defined between the hot and cold channels as well as on the outside of the cold channel. Inflows $T_{\text{cold}} = 10$ °C and $T_{\text{hot}} = 50$ °C are defined at the ends of the channels.

Fluid flow simulation is performed using *Laminar Flow*. No slip walls are specified between the channels and on the outside of the cold channel. Slip walls are specified in the porous section. Inlets $\dot{V}_{\text{hot}}$ and $\dot{V}_{\text{cold}}$ are defined for the channels as well as an outlet with $p = 0$ Pa. Initial values for velocity inside the channels are set to the inlet velocities. The fluid and heat modules are coupled together using the *Nonisothermal Flow* multiphysics module. A stationary study was then performed. The temperature distribution and velocity profile are plotted in figures 1 and 2.

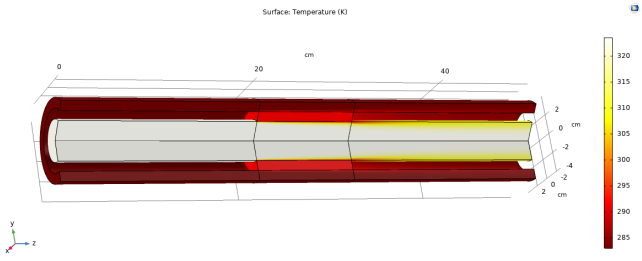

Figure 1: Reference solution temperature distribution.

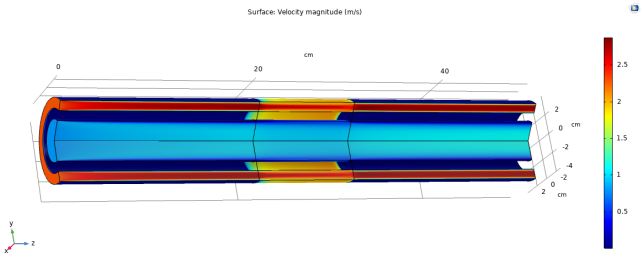

Figure 2: Reference solution velocity field.

One way of testing the effectiveness of the heat transfer is to define a ratio between the temperatures of the channel inlets and outlets as [1, p. 687]

$$\varepsilon = \frac{T_{\text{cold out}} - T_{\text{cold in}}}{T_{\text{hot in}} - T_{\text{cold in}}}. \tag{1}$$

The higher the value, the better the heat exchanger. For our reference simulation this is

$$T_{\text{cold out}} = 284.13 \text{ K}, \; T_{\text{hot out}} = 316.92 \text{ K},$$
$$\varepsilon_{\text{ref}} = \frac{284.13 - 273.15}{316.92 - 273.15} = 0.029.$$

Another characterizing value is the pressure drop in the hot channel

$$\Delta p_{\text{ref}} = 0.419 \text{ Pa}.$$

A lower pressure drop would mean less resistance to fluid flow.

3 Microscale modelling of porous medium

The goal is to design a microstructure that transfers as much heat as possible in the radial direction while still allowing fluid to flow through it. This would be a structure with high radial thermal conductivity and high axial permeability. If the porous material is assumed to consist of ellipsoidal particles, then we have three basic options with different levels of symmetry.

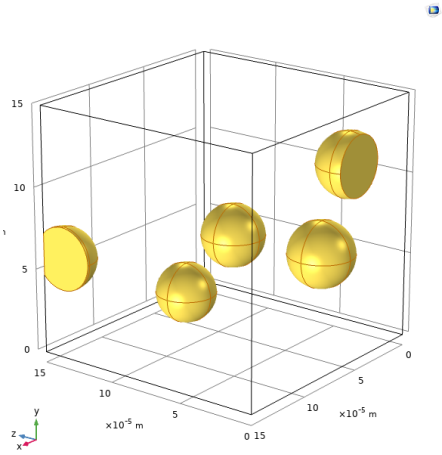

Figure 3: Microstructure A.

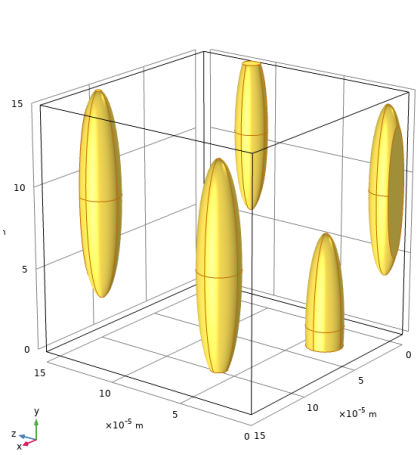

Figure 4: Microstructure B.

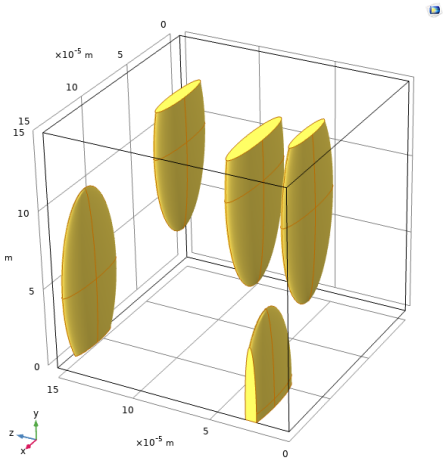

Figure 5: Microstructure C.

Structure	r_a	r_b	r_c
A	20 µm	r_a	r_a
B	12 µm	60 µm	r_a
C	30 µm	60 µm	5 µm

Table 1: Microstructure dimensions.

We can determine the macroscale properties of these microstructures using homogenization [2, p. 149]. Properties for these structures can be calculated as [3]

$$\kappa = \frac{u\mu a}{\Delta p}, \; k = \frac{qa}{T_{\text{hot}} - T_{\text{cold}}}, \; \phi = \frac{V_{\text{fluid}}}{V_{\text{tot}}}, \tag{2}$$

where κ is permeability, u is the average outlet velocity, μ is viscosity, a is unit cell size, k is thermal conductivity, q is average outlet heat flux and ϕ is porosity.

A microscale geometry generator was used in COMSOL to generate the structures A, B and C. Separate fluid and heat simulations need to be performed on the microscale models to determine their properties. *Creeping flow* was used for fluid simulation. An inlet with a low velocity and an outlet with $p =$ Pa were set on the x-axis. *Heat Transfer in Solids and Fluids* was used for heat simulations. Temperatures T_{hot} and T_{cold} were set to opposing faces on the y-axis. Other configurations are the same as in section 2.

Structure	$k_x \left(\frac{\text{W}}{\text{m K}}\right)$	$k_y \left(\frac{\text{W}}{\text{m K}}\right)$	$k_z \left(\frac{\text{W}}{\text{m K}}\right)$	$\kappa_x(\mu\text{m}^2)$	$\kappa_y(\mu\text{m}^2)$	$\kappa_z(\mu\text{m}^2)$	ϕ
A	k_y	0.0334	k_y	1040	κ_x	κ_x	0.965
B	0.0318	0.119	k_x	734	1628	κ_x	0.956
C	0.0620	0.230	0.0290	1170	966	658	0.958

Table 2: Thermal conductivity k, permeability κ and porosity ϕ for different microstructures, $a = 150$ µm.

Simulations were performed for different geometries with cell size $a = 150$ µm, number of inclusions $n = 5$, porosity $\phi \approx 0.96$. Each property is calculated three times with a new random geometry. The results of these simulations were assembled in table 2.

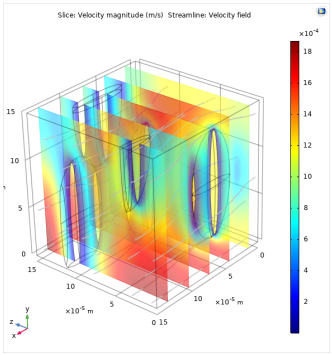

Figure 6: Microstructure C x orientation velocity field.

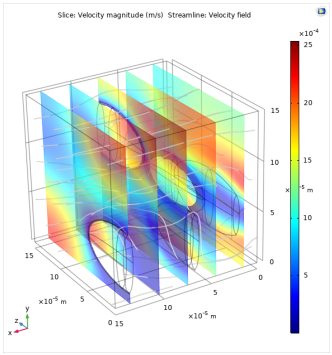

Figure 7: Microstructure C z orientation velocity field.

It can be seen that by increasing the length of an ellipsoid on an axis causes the thermal conductivity on that axis to increase. Thermal conductivity of a porous medium can be calculated from the conductivities of the solid and fluid as [3, p. 544]

$$k = \phi k_f + (1 - \phi)k_s. \tag{3}$$

The effect of anisotropy on permeability can be seen from figures 6 and 7. In the z orientation the structure has a larger surface area in the direction of the flow.

n = 5			a = 150 µm			
$a(\mu\text{m})$	$k_y \left(\frac{\text{W}}{\text{m K}}\right)$	$\kappa_x(\mu\text{m}^2)$	n	$k_y \left(\frac{\text{W}}{\text{m K}}\right)$	$\kappa_x(\mu\text{m}^2)$	ϕ
80	0.0318	38.7	5	0.0334	1040	0.965
150	0.0334	1040	10	0.0457	135	0.904
600	0.0341	18500	20	0.108	96.3	0.821
1000	0.0343	34400	40	0.320	43.9	0.696

Table 3: Properties for microstructure A at different cell scale a and inclusion number n.

The impact of unit cell size a and number of inclusions n can now be investigated. Simulations were performed on structure A by varying unit cell size and number of inclusions, as can be seen in table 3. The final properties for A, B and C are presented in table 4.

Structure	$k_x \left(\frac{\text{W}}{\text{m K}}\right)$	$k_y \left(\frac{\text{W}}{\text{m K}}\right)$	$k_z \left(\frac{\text{W}}{\text{m K}}\right)$	$\kappa_x(\mu\text{m}^2)$	$\kappa_y(\mu\text{m}^2)$	$\kappa_z(\mu\text{m}^2)$	ϕ	$a(\mu\text{m})$	n
A	k_y	0.0296	k_y	705000	κ_x	κ_x	0.988	3000	10
B	0.0284	0.0649	k_x	257000	747000	κ_x	0.990	3000	10
C	0.0456	0.125	0.0281	349000	461000	264000	0.988	3000	10

Table 4: Final determined properties for A, B, C.

4 Macroscale simulation of heat exchanger with porous medium

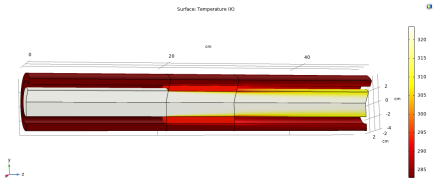

Figure 8: Microstructure A heat exchanger temperature distribution.

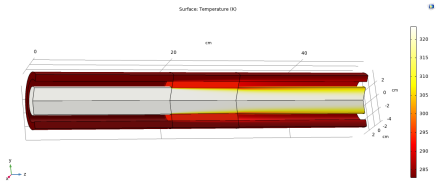

Figure 9: Microstructure B heat exchanger temperature distribution.

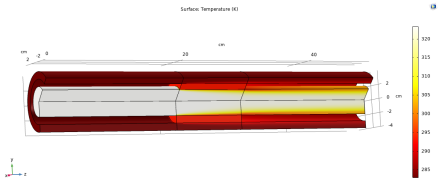

Figure 10: Microstructure C heat exchanger temperature distribution.

The model from section 2 is now modified for porous domain simulation. A *Fluid and Matrix Properties* component is added to the *Laminar Flow* module. The volume fraction and permeability is set with the radial part approximated as $\kappa_r = \sqrt{\kappa_x^2 + \kappa_y^2}$. In the heat transfer module, the *Porous Medium* component is set with the thermal conductivity the same way. Thermal conductivity for the fluid is set to 0 and volume fraction to 1. Density and specific heat capacity were then calculated for porous medium similarly to equation 5 [4].

The microstructures specified in table 4 are simulated for each type, after which the effectivess and pressure drop are determined. The temperature distributions are presented in figures 8, 9 and 10. Graphs comparing the structures are plotted in figures 11 and 12.

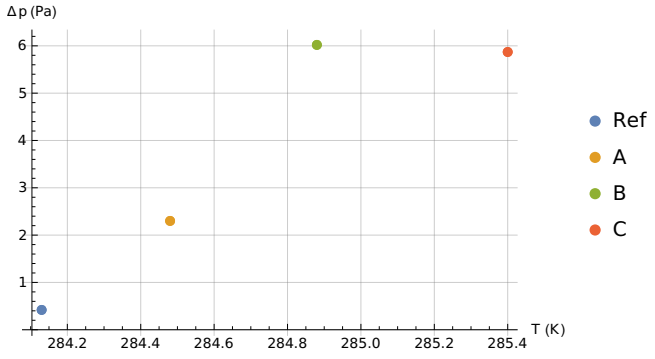

Figure 11: Temperature vs. pressure drop.

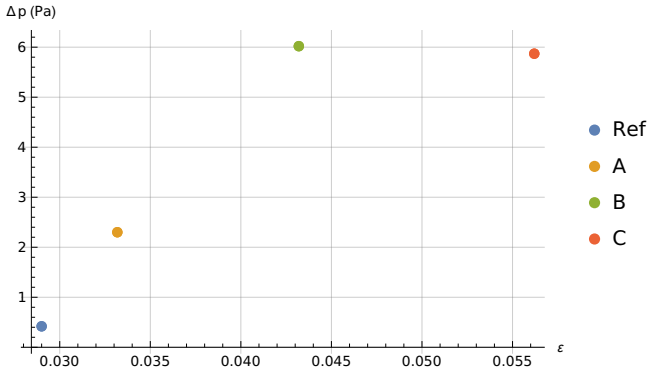

Figure 12: Effectiveness vs. pressure drop.

5 Conclusion

It can be seen in figure 11 that the pressure drop in relation to the temperature is lower compared to the other types. This would suggest that structure C is the most effective of the tested microstructures. The exact properties of C are not necessarily optimal however, as this would require further optimization. Futhermore, the accuracy of the simulation results was seen to vary a lot between runs, so getting a larger sample would be beneficial.

Acknowledgements

The author wishes to thank Ari Salmi, Patrick Grahn, Joni Mäkinen and Oskari Tommiska for the topic and for providing the microscale generator.

References

[1] Incropera, F. P., DeWitt, D. P., Bergman, T. L. & Lavine, A. S. Fundamentals of Hean and Mass Transfer. Wiley, 6th ed., 2007.

[2] Mäkinen, J. & Tommiska, O. COMSOL Reference Guide For the Courses Finite element modelling for physicists I & II (MATR378, MATR379). University of Helsinki, 2020.

[3] Bejan, A. Convection Heat Transfer. Wiley, 4th ed., 2013.

[4] Heat Transfer Module User's Guide. COMSOL, 2018.